Chinese Journal of Chemistry, **2006**, *24*, 750—754

Full Paper

Reactions of Laser Ablated Metal Plasma with Molecular Alcohol Beams: Dependence of the Produced Cluster Ion Species on the Beam Condition

NIU, Dong-Mei(牛冬梅) LI, Hai-Yang*(李海洋) ZHANG, Shu-Dong(张树东)

Dalian Institute of Chemical Physics, Chinese Academy of Sciences, Dalian 116023, China
Key Laboratory of Environmental Optics and Technology, Anhui Institute of Optics and Fine Mechanics, Chinese Academy of Sciences, Hefei 230031, China

The gas phase reactions of metal plasma with alcohol clusters were studied by time of flight mass spectrometry (TOFMS) using laser ablation-molecular beam (LAMB) method. The significant dependence of the product cluster ions on the molecular beam conditions was observed. When the plasma acted on the low density parts of the pulsed molecular beam, the metal-alcohol complexes M^+A_n (M＝Cu, Al, Mg, Ni and A＝C_2H_5OH, CH_3OH) were the dominant products, and the sizes of product ion clusters were smaller. While the plasma acted on the high density part of the beam, however, the main products turned to be protonated alcohol clusters H^+A_n and, as the reactions of plasma with methanol were concerned, the protonated water-methanol complexes $H_3O^+(CH_3OH)_n$ with a larger size ($n\leqslant 12$ for ethanol and $n\leqslant 24$ for methanol). Similarly, as the pressure of the carrier helium gas was varied from 1×10^5 to 5×10^5 Pa, the main products were changed from M^+A_n to H^+A_n and the sizes of the clusters also increased. The changes in the product clusters were attributed to the different formation mechanism of the output ions, that is, the M^+A_n ions came from the reaction of metal ion with alcohol clusters, while H^+A_n mainly from collisional reaction of electron with alcohol clusters.

Keywords metal plasma, alcohol cluster, laser ablation, time of flight mass spectrometry

Introduction

Numerous studies on the chemical reactions of transition metal ions with various molecular clusters in the gas phase have been carried out to clarify the catalytic activity of metal ions and the mechanisms in many important organometallic reactions.[1-7] The study of gas phase chemistry of these ions can provide intrinsic chemical and physical properties, and can contribute to a better understanding of their behavior in condensed phase. Methanol and ethanol are widely used chemicals and often methanol emerges as a reaction intermediate and a precursor in synthesis, decomposition, and oxidation reactions involving hydrocarbons. There are many literature data about the reaction of their molecules and clusters with alkaline and transition metals.[8-17] In these combined metal-alcohol systems, the principal cluster series have been presented as M^+A_n, and for some of the systems, evidence of the H-elimination of M^+A_n has been reported. Lu and coworkers[8,12] studied the reactions of alkaline earth metal ions with methanol clusters in the ion detector chamber using laser ablation-molecular beam method and reported the H-elimination products of metal-methanol complexes. Koo[15] studied the intracluster ion-molecule reactions of Ti^+ with ethanol and *t*-butanol clusters and reported the H-elimination products. Farrar[17] reviewed the reaction of the alkaline earth metal ions of Mg^+, Ca^+, and Sr^+ with some polar solvent molecules such as CH_3OH and their deuterium products, and reported the hydrates of these metal ions. The metal ions in the experiments mentioned above were generated from laser-ablated plasma from a metal target, either in the source chamber or the detection chamber of the TOFMS, and diffused to the vacuum without further restriction.

In the present work, by introducing a reaction cell out side the pulsed valve in the source chamber of TOFMS, we hope to increase the probability of the collision induced reaction to see if there are some new phenomena when alcohol beams act with the metal plasma. Actually, we found the very interesting dependence of the sizes and species of the output cluster ions on the molecular beam density, which reflects the different origination of these ions, as will be discussed in detail.

Experimental

A schematic diagram of the LAMB/TOFMS is shown in Figure 1, consisting of two differentially

* E-mail: hli@dicp.ac.cn; Tel.: 0086-411-84379509
Received September 1, 2005; revised December 2, 2005; accepted January 11, 2005.
Project supported by the the National Natural Science Foundation of China (No. 20573111) and 863 Project (No. 2005AA641020).

pumped chambers: the source chamber and the detection chamber. Reactant CH_3OH or C_2H_5OH seeded in helium with a backing pressure of 0.1—0.5 MPa was introduced through a pulsed valve (General valve with 0.8 mm orifice diameter, opening time 300 μs) to the source chamber, which was pumped by a 1500 L/s diffusion pump. After passing the valve, the mixture gases went through a reaction cell with inner diameter of 2 mm and length of 30 mm, where they reacted with the metal plasma. The plasma was generated by the second harmonic output at 532 nm of a Q-switched Nd: YAG laser (25 ns pulse width) to strike the rotating solid metal target located 20 mm downstream from the nozzle. The laser beam was weakly focused to a spot of 1 mm^2 by a 500 mm focal length lens. The laser flux at the target surface was varied in the range of 20—50 mJ/pulse. The resulting ions were skimmed by a 2 mm conical skimmer and cooled down as they traveled to the detection chamber, which was pumped by a 1200 L/s turbo-molecular pump, with the distance of 90 mm from nozzle to skimmer. The resulting pulsed beam entered the extraction region of a TOFMS, placed 90 mm from the skimmer. Under the inlet frequency of 10 Hz, the pressures in the source and detection chambers were about 1×10^{-2} and 3×10^{-4} Pa respectively.

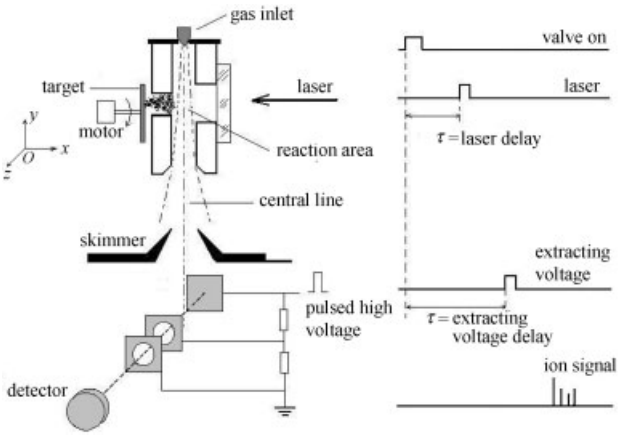

Figure 1 Schematic diagram of the experimental setup for the coupling of a laser ablation-molecular beam source with an orthogonal time-of-flight mass spectrometer.

The positive and negative ions that were produced directly from the reaction of plasma and the sample gas were studied without further use of ionization. Following a delay of typical 80—200 μs after the laser shot, the ions were extracted by 1150 V pulsed electric field applied to the repeller. The ion extraction pulse has a rise time of 100 ns, and the accelerated ions then traveled through a 500 mm long field-free region, which was terminated at a double microchannel plate detector. The mass spectra were recorded by a 1 G/s 100 MHz digital oscilloscope coupled with a personal computer and by a cumulative collection of 128 laser shots at a repetition of 10 Hz. Analytical grade CH_3OH, C_2H_5OH, and metal target of Ni and Cu (99.5%) were used without further purification.

Results and discussion

Dependence of the product cluster ion species on the laser delay and the pressure of the carrier gas

By fixing the pressure of carrier gas at 0.2 MPa and setting the delay τ_1 of the laser shots to the opening of pulsed valve at 0.44 and 0.92 ms, two typical mass spectra of nickel plasma reaction with methanol were got and shown in Figure 2. As we can see, the main products in Figure 2a are metal-methanol complex clusters of $Ni^+(CH_3OH)_{9-15}$ and protonated methanol clusters of $H^+(CH_3OH)_{7-12}$. While the delay τ_1 was set at 0.92 ms, the dominant clusters were changed to $H^+(CH_3OH)_{14-23}$ and protonated water-methanol cluster $H_3O^+(CH_3OH)_{13-21}$ of much larger sizes and much weaker intensities, as shown in Figure 2b. An overall dependence of the resulting clusters on the laser delay is displayed in Figure 3, which was obtained when 0.2 MPa helium was used as carrier gas. As τ_1 was increased from 0.33 to 0.46 ms, the sizes of the clusters increased, while τ_1 was changed from 1.12 to 1.52 ms, the cluster sizes were decreased.

To investigate if this dependence on delay time was universal in the experiments by the present method, the

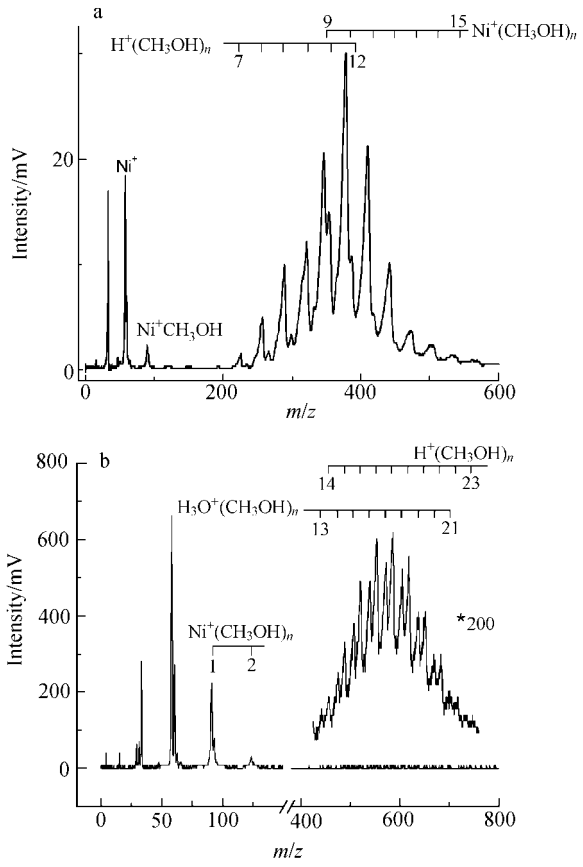

Figure 2 Time of flight mass spectrum obtained from reaction of Ni plasma with methanol at carrier gas pressure of 0.2 MPa and laser shot delay of 0.44 (a) and 0.92 ms (b).

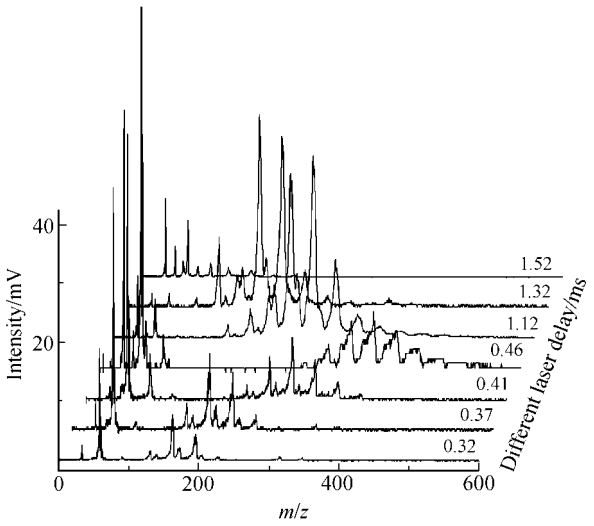

Figure 3 Time of flight mass spectra obtained from reaction of Ni plasma with methanol at different laser delay of 0.33—1.52 ms, and the backing pressure of helium is 0.2 MPa.

nickel target was firstly replaced with aluminum, magnesium and copper target one by one, and methanol was substituted with ethanol to repeat the experiment procedure. To our expectation, the produced ion clusters displayed the same trends to the laser delay, *i.e.* the metal-alcohol complex clusters M^+A_n and protonated alcohol clusters H^+A_n of relatively small sizes were the main ion species at the small and large τ_1 values, while H^+A_n and $H_3O^+A_n$ of large sizes characterized the mass spectra at moderate τ_1 values. Four typical mass spectra of Cu plasma reacted with ethanol at backing pressure of 0.2 MPa are shown in Figure 4 to illustrate the similarity. When τ_1 was 0.4 ms (a), the main products were $Cu^+(C_2H_5OH)_n$ and $H^+(C_2H_5OH)_n$ of small sizes ($n\leqslant 6$) and equivalent intensities. The highest peak corresponds to $H^+(C_2H_5OH)_5$. When τ_1 was 0.44 ms, however, the $Cu^+(C_2H_5OH)_n$ clusters ($n\leqslant 8$) became the dominant product with the highest peak of $Cu^+(C_2H_5OH)_6$. As τ_1 was increased to 0.48 ms, the main products were switched to the $H^+(C_2H_5OH)_n$ series ($n\leqslant 11$) . As τ_1 went on increasing, the sizes of the cluster ions were increased ($n\leqslant 12$) while the intensities decreased apparently. The highest peak of the $Cu^+(C_2H_5OH)_n$ series corresponded to $n=4$, 5, 7, 8 in a, b, c, d respectively. Similar to Ni-methanol reaction, no magic number was recognized.

Since the different laser delay time τ_1 means that the laser ablated metal plasma interacts with the different parts of the beam, *i.e.*, small τ_1 will correspond to that the plasma can interact with the front part of the molecular beam, while large τ_1 will correspond to that the plasma can interact with the tail of the beam, and moderate values of τ_1 mean that the interactions take place at the middle densest part of the beam. Naturally, the changes of the sizes and species of the resulting clusters can be speculatively associated with the local density of the molecular beam, which will be varied at the different parts of the beam.

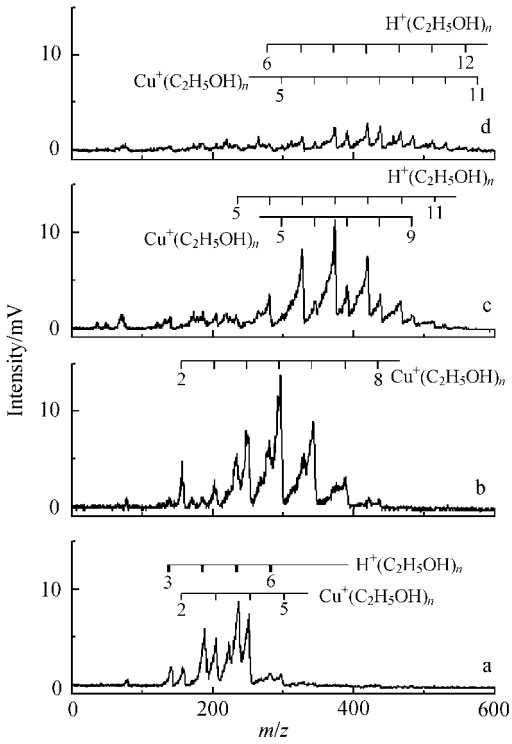

Figure 4 Time of flight mass spectra obtained from reaction of Cu with ethanol at different laser delay time: (a) 0.40, (b) 0.44, (c) 0.48, and (d) 0.50 ms, and the backing pressure of helium 0.2 Mpa.

As varying the pressure of the carrier gas was an efficient way to change the local density of the beam, the Cu-ethanol reaction was repeated at four different backing pressures of 0.2, 0.3, 0.4 and 0.5 MPa with the laser delay fixed at 0.46 ms, while the time of flight mass spectra are displayed in Figure 5.

The intensities and sizes of the output cluster ions were changed with either the laser delay or the pressure of the carrier gas. It is instructive to see how the density was distributed in the pulsed molecular beam. Clusters were well known able to be efficiently generated when the pulsed molecular beam passed through the nozzle. In the head of the beam ($\tau_1=0.33$—0.42 ms), the density of the mixed reactant and carrier gas was relatively small, and the size of the reactant clusters was small. In the middle part ($\tau_1=0.42$—1.02 ms), the density and the size became much larger, while at the tail of the beam ($\tau_1=1.02$—1.52 ms), these variables once again became smaller. The incremental ionic cluster sizes when τ_1 was increased from 0.32 to 0.46 ms or decremental cluster sizes when τ_1 was increased from 0.46 to 1.52 ms in Figure 4 were consistent with the size distribution of the clusters in the beam.

To manifest the changes of the signal intensity, the following process should be considered. When the laser ablated plasma acted on the head and the tail part of the beam where the local density was relatively low, both the metal ions and the hot molecules had a longer free

path, and could reach the central line of the reaction cell and collide with the reactant gas to form some small-sized metal-alcohol complexes. When the plasma acted on the much denser middle part of the beam, the M^+could barely touch the reactant molecules, and the intensities of the M^+A_n clusters were decreased greatly. As to electrons, because of their longer free paths, some of them could still reach the central line to react with the alcohol gas to form the protonated clusters. Hence the drop of the intensities of H^+A_n was not so sharp as that of M^+A_n. When the carrier pressure went up from 0.2 to 0.6 MPa, the same part of the beam was to become denser and the products were to undergo a transformation from M^+A_n and H^+A_n to H^+A_n .

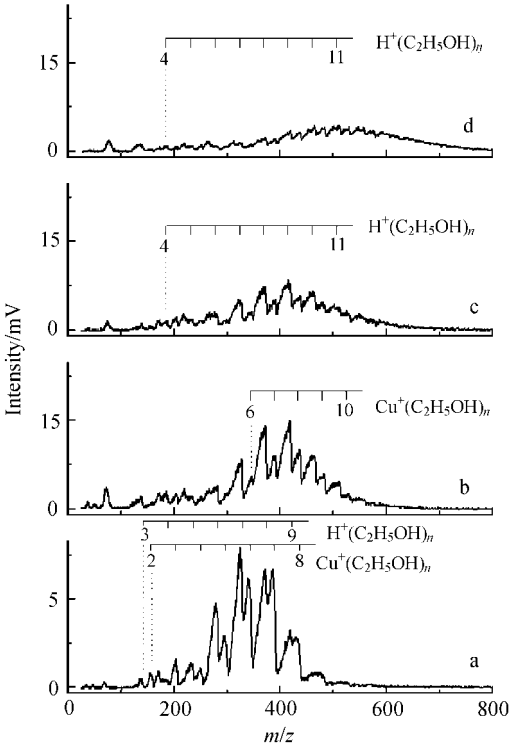

Figure 5 Time of flight mass spectra obtained from reaction of Cu with ethanol at different pressure of carrier gas: (a) 0.2, (b) 0.3, (c) 0.4, (d) 0.5 MPa, and the laser delay τ_1 of 0.46 ms.

The reaction of Cu plasma with ethanol beam backed by carrier gas of 0.2—0.5 MPa is illustrated in Figure 5. Seen from spectrum a, the main resulting clusters are metal-ethanol complex clusters $Cu^+(C_2H_5OH)_n$ and protonated ethanol clusters $H^+(C_2H_5OH)_n$ of equivalent intensities at 0.2 MPa. When the pressure was set at 0.3 MPa (b), the intensities of $Cu^+(C_2H_5OH)_n$ series were decreased evidently and $H^+(C_2H_5OH)_n$ became the dominant products. When the pressure went on to 0.4 MPa (c), the overall intensities of the mass spectra were decreased. When the pressure was set at 0.5 MPa (d), the intensities were weakened apparently together with a deteriorated resolution, and the only discriminable series was $H^+(C_2H_5OH)_n$. When the pressure was raised further higher, the whole spectrum became undistinguishable (not shown in the Figure 5) and the intensity was decreased monotonously.

Reaction mechanism

It has been generally accepted that the metal alcohol complexes stem from the association reaction between the metal ions and alcohol clusters, while the association products are probably stabilized by evaporation of one or more molecules or by collision with the carrier gas.[12,15]

$$M^+A_m \rightarrow M^+A_n + A_{m-n} \quad (n < m-1) \tag{1}$$

As in some other researches, the formation of the protonated methanol or ethanol clusters is mostly due to the collision of electrons with the methanol or ethanol clusters companied with evaporation of one or more molecules.[15,18]

$$e + (C_2H_5OH)_m \rightarrow H^+(C_2H_5OH)_n + C_2H_5O(C_2H_5OH)_{m-n-1} + 2e \quad (n \leqslant m-1) \tag{3}$$

$$e + (CH_3OH)_m \rightarrow H^+(CH_3OH)_n + CH_3O(CH_3OH)_{m-n} + 2e \quad (n \leqslant m-1) \tag{4}$$

The probable pathways for the formation of the protonated water-methanol clusters are the combination of methanol with protonated water to arise from the multi-collision of the metal plasma and the methanol, and the intra-cluster elimination of a neutral dimethyl ether CH_3OCH_3 from the $H^+(CH_3OH)_m$ clusters:[19]

$$H^+(CH_3OH)_m \rightarrow H_3O^+(CH_3OH)_{m-2} + CH_3OCH_3 \tag{5}$$

Conclusion

The gas phase reaction of metal plasma with alcohol clusters was studied by LAMB method. Cluster ions of M^+A_n, H^+A_n (A=CH_3OH, C_2H_5OH) and $H_3O^+(CH_3OH)_n$ were detected. Dependences of the species and sizes of the product clusters on the laser shot delay and on the pressure of the carrier gas were attributable to the distribution of local density in the beam.

References

1 Barran, P. E.; Mikhailov, V.; Stace, A. J. *J. Phys. Chem. A* **1999**, *103*, 8792.
2 Rodgers, M. T.; Walker, B.; Armentrout, P. B. *Int. J. Mass Spectrom.* **1999**, 1*82/183*, 99.
3 Caraiman, D.; Bohme, D. K. *J. Phys. Chem. A* **2002**, *106*, 9705.
4 Rue, C.; Armentrout, P. B.; Kretzschmar, I.; Schroder, D.; Schwarz, H. *J. Phys. Chem. A* **2002**, *106*, 9788.
5 Higashide, H.; Oka, T.; Kasatani, K.; Shinohara, H.; Sato, H. *Chem. Phys. Lett.* **1989**, *163*, 485.
6 Schröder, D.; Weiske, T.; Schwarz, H. *Int. J. Mass Spectrom.* **2002**, *219*, 729.

7 Zhang, Q.; Kemper, P. R.; Bowers, M. T. *Int. J. Mass Spectrom*. **2001**, *210/211*, 265.
8 Lu, W. Y.; Huang, R. B.; Yang, S. H. *J. Phys. Chem*. **1995**, *99*, 12099.
9 Draves, J. A.; Lisy, J. M. *J. Am. Chem. Soc*. **1990**, *112*, 9006.
10 Woodward, C. A.; Dobson, M. P.; Stace, A. J. *J. Phys. Chem. A* **1997**, *101*, 2279.
11 Zhang, X.; Castleman, A. W. Jr. *J. Am. Chem. Soc*. **1992**, *114*, 8607.
12 Lu, W. Y.; Yang, S. H. *J. Phys. Chem. A* **1998**, *102*, 825.
13 Oliveira, M. C.; Marcalo, J.; Vieira, M. C.; Ferreiraac, M. A. A. *Int. J. Mass Spestrom*. **1999**, *185*, 825.
14 Koo, Y. M.; An, H. J.; Yoo, S. K.; Jung, K. W. *Int. J. Mass Spestrom*. **2003**, *226*, 305.
15 Koo, Y. M.; Kim, J. H.; Choi, Y. K.; Lee, H.; Jung, K. W. *J. Phys. Chem. A* **2002**, *106*, 2465.
16 Kaya, T.; Horiki, Y.; Kobayashi, M.; Shinohara, H.; Sato, H. *Chem. Phys. Lett*. **1992**, *200*, 435.
17 Farrar, J. M. *Int. Rev. Phys. Chem*. **2003**, *22*, 593.
18 Vadyanathan, G.; Coolbaugh, M. T.; Peifer, W. R.; Garvey, J. F. *J. Chem. Phys*. **1991**, *94*, 1850.
19 Morgan, S.; Keesee, R. G.; Castleman, A. W. Jr. *J. Am. Chem. Soc*. **1989**, *111*, 3841.

(E0509011 LI, L. T.; LING, J.)